DALTON
FULL PAPER

Sterically hindered iminophosphorane complexes of vanadium, iron, cobalt and nickel: a synthetic, structural and catalytic study †

Sarah Al-Benna,[a] Mark J. Sarsfield,[a] Mark Thornton-Pett,[a] Daniel L. Ormsby,[a] Peter J. Maddox,[b] Philippe Brès[b] and Manfred Bochmann *[c]

[a] *School of Chemistry, University of Leeds, Leeds, UK LS2 9JT*
[b] *BP Amoco Chemicals Ltd., Sunbury Research Centre, Chertsey Road, Sunbury-on-Thames, UK TW16 7LN*
[c] *School of Chemical Sciences, University of East Anglia, Norwich, UK NR4 7TJ*

Received 3rd August 2000, Accepted 27th September 2000
First published as an Advance Article on the web 6th November 2000

Bis(aryliminophosphoranyl)alkanes $L^1 = (CH_2)_n(R^1{}_2P{=}NR^2)_2$ (n = 1 or 2, R^1 = Ph or Me, R^2 = Ph, $C_6H_2Me_3$-2,4,6 or $C_6H_3Pr^i{}_2$-2,6) reacted with cobalt and nickel dihalides to give chelate complexes of the type $MX_2(L^1)$. The reaction of $Li[HC(Ph_2P{=}NR^2)_2]$ with MX_2 afforded the compounds $MX\{HC(Ph_2P{=}NR^2)_2\}$ (M = Co, X = Cl; M = Ni, X = Br). The crystal and molecular structures of $CoCl_2\{CH_2(Ph_2P{=}NPh)_2\}$ and $NiBr\{HC(Ph_2P{=}NC_6H_3Pr^i{}_2)_2\}$ were determined. While the former has the expected tetrahedral structure, the latter is square planar. *Ab initio* calculations on the latter show that the bonding of the bis(iminophosphoranyl)methanide ligand to nickel involves π delocalisation over the N_2P_2C framework as well as σ bonding between nickel and the P_2CH carbon atom. Bis(iminophosphoranyl)pyridines $C_5H_3N(R_2P{=}NR')_2$-2,6 (R = Ph or cyclohexyl, R′ = $C_6H_2Me_3$-2,4,6, $C_6H_3Pr^i{}_2$-2,6 or $SiMe_3$) reacted with $VCl_3(thf)_3$, FeX_2 (X = Cl or Br) or $CoCl_2$ to give the corresponding octahedral (V) or five-co-ordinate (Fe, Co) complexes. The crystal structure of $FeBr_2\{C_5H_3N(Ph_2P{=}NSiMe_3)_2$-2,6$\}$ has been determined; the complex is trigonal bipyramidal. In the presence of methylaluminoxane $[MeAlO]_n$, cobalt complexes of bis(aryliminophosphoranyl)methane are moderately active in ethene polymerisation, while bis(iminophosphoranyl)pyridine iron complexes show only low activity. The vanadium complexes polymerise ethene under ambient conditions and give polymers of very high molecular weight.

Introduction

Nitrogen ligands with bulky substituents are currently attracting substantial interest as tools for tailoring the co-ordination gap aperture, and hence the reactivity, of metal complexes, especially as a means for developing non-metallocene catalysts for the polymerisation of olefins.[1] Diazabutadienes[2,3] and bis(imino)pyridines[4] are particularly noteworthy in this context. It has been shown that the rates of both chain propagation and of termination are highly sensitive to the substitution pattern of aryl substituents, with bulky derivatives leading to high molecular weight polyolefins, while sterically less demanding analogues produce oligomers.[5] These results underline above all the importance of steric factors in ligand design.

We have become interested in devising ligands that offer a steric environment similar to diimines, while the electronic characteristics, such as donor strength and π-acceptor capacity, are clearly different. Iminophosphoranes $X{-}PR_2{=}NR'$ constitute a class of readily accessible ligands suitable for such a study (X = amino or alkyl; R, R′ = alkyl, aryl or silyl). An early representative of this class is Keim's iminophosphorane amidato complex $Ni(\eta^3\text{-}C_3H_5)\{(Me_3Si)_2N(allyl)P(NSiMe_3)_2\}$, a single-component ethene polymerisation catalyst and, to our knowledge, the first example to demonstrate the importance of bulky nitrogen chelates in polymerisation catalysis.[6] There are numerous complexes of bis(iminophosphoranyl)methanes (**A**) and of the corresponding anions (**B**), particularly of rhodium, iridium, palladium and platinum, where co-ordination geometries of the type shown in structures **C**–**F** are found (Chart I).[7–9] The co-ordination chemistry of iminophosphoranylphosphines has similarly attracted attention.[10] Here we report on the complexes of vanadium and Group 8–10 first row metals with bis(aryliminophosphoranyl)methanes (**I**, **II**), 1,2-bis(aryliminophosphoranyl)ethanes (**III**, **IV**), the bis(aryliminophosphoranyl)methanide anion (**I** − H, **II** − H), and bis(aryliminophosphoranyl)pyridines (**V**, **VI**) (Chart II). The unusual reaction of ligands of type **III** with $TiCl_4$ has recently been published as a preliminary communication.[11a]

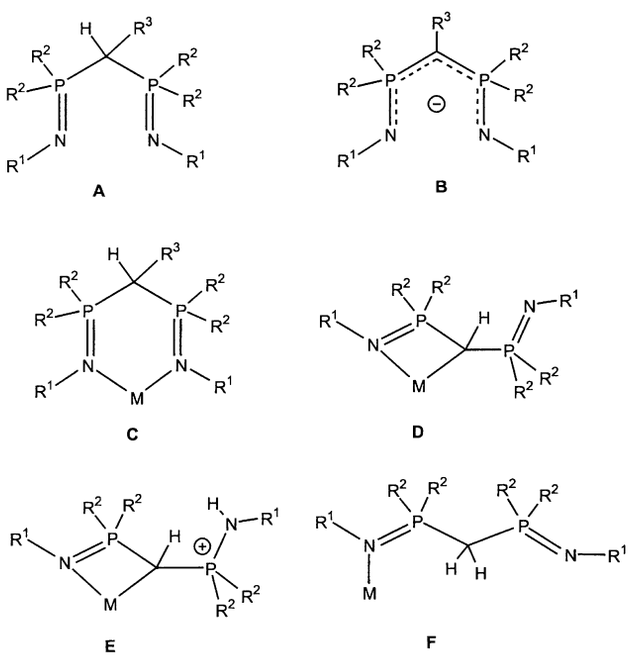

Chart I

† Dedicated to Professor H. W. Roesky on the occasion of his 65th birthday.

Electronic supplementary information (ESI) available: syntheses of ligands, positional parameters used for MO calculations. See http://www.rsc.org/suppdata/dt/b0/b006329k/

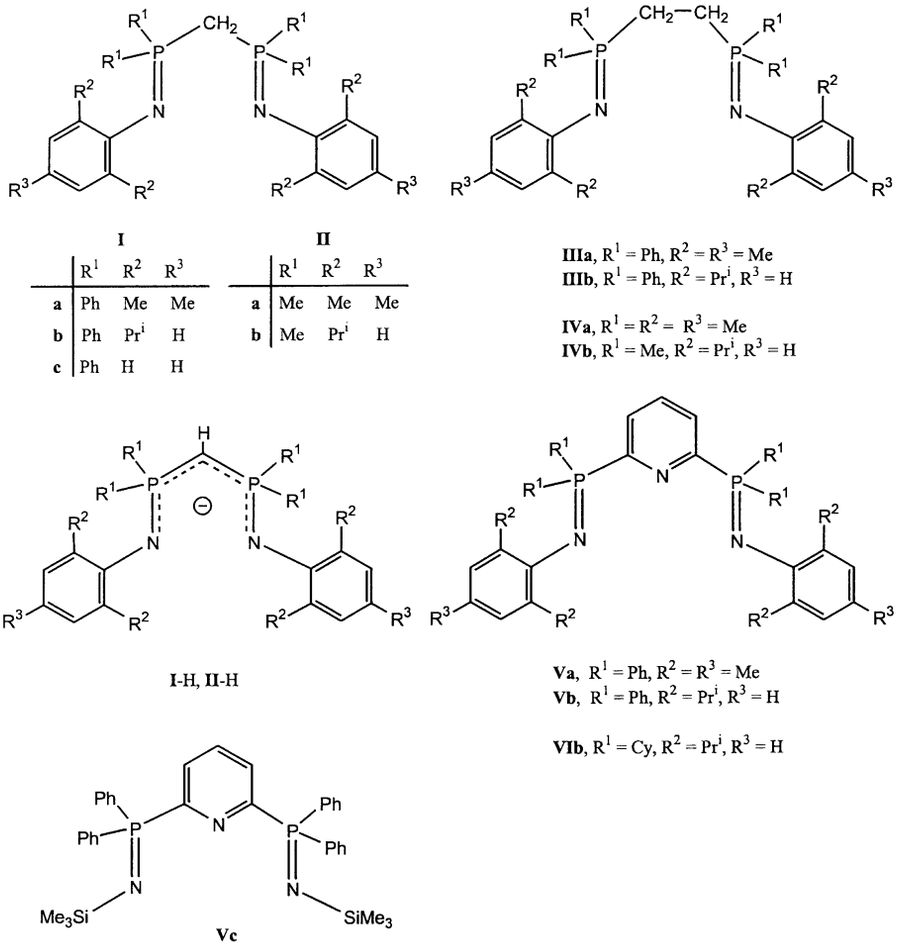

	R1	R2	R3
a	Ph	Me	Me
b	Ph	Pri	H
c	Ph	H	H

	R1	R2	R3
a	Me	Me	Me
b	Me	Pri	H

Chart II

Results and discussion

Ligand synthesis

The ligands $CH_2(Ph_2P{=}NAr)_2$ **I** (Ar = 2,4,6-$Me_3C_6H_2$ **a**, 2,6-$Pr^i_2C_6H_3$ **b** or Ph **c**) were readily prepared in high yield by treating bis(diphenylphosphino)methane (dppm) with the corresponding aryl azides in toluene at 60 °C over a period of 4 h.[7] The formation of the dimethylphosphino analogues **IIa** (Ar = 2,4,6-$Me_3C_6H_2$) and **IIb** (Ar = 2,6-$Pr^i_2C_6H_3$), the 1,2-bis(diphenylphosphino)ethane (dppe) derivative **IIIb**, and the 1,2-bis(dimethylphosphino)ethane (dmpe) compounds **IVa** and **IVb** was more facile, and reactions were complete within 30 min (Chart II). The compounds are crystalline solids.

2,6-Bis(diphenylphosphino)pyridine was prepared from $NaPPh_2$ and 2,6-difluoropyridine in liquid ammonia following McFarlane's method[12] but in substantially improved yield (93%, compared to 40%[12]). Oxidation with 2,4,6-$Me_3C_6H_2N_3$ and 2,6-$Pr^i_2C_6H_3N_3$ affords the ligands **Va** and **Vb**, respectively (R^1 = Ph). The new compound 2,6-bis(dicyclohexylphosphino)-pyridine was made from $LiPCy_2$ (Cy = cyclohexyl) and 2,6-difluoropyridine in tetrahydrofuran (thf) in 65% yield. It is readily oxidised by 2,6-$Pr^i_2C_6H_3N_3$ to give **VIb** (Scheme 1).

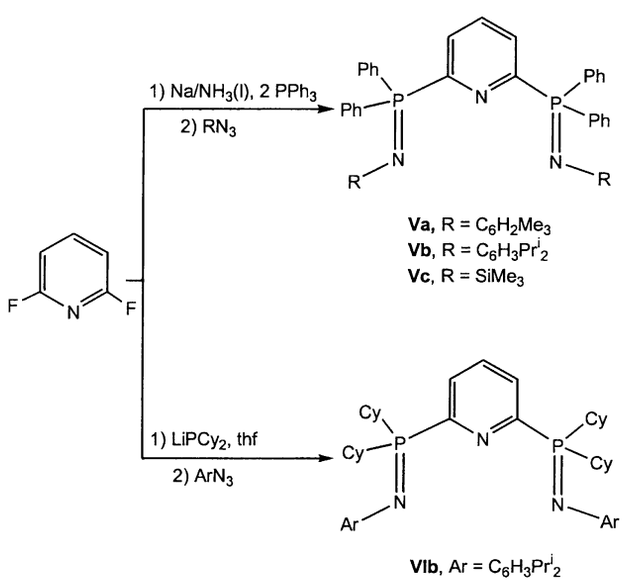

Scheme 1

Bis(aryliminophosphoranyl)alkane complexes

Adding ligands **I** to a suspension of anhydrous cobalt(II) chloride in thf at room temperature leads to an immediate colour change. On stirring for a few hours the adducts $CoCl_2$(**Ia**) to $CoCl_2$(**Ic**) are obtained as pale blue powders. Similarly, the reaction of $NiBr_2$(dme) (dme = 1,2-dimethoxyethane) affords the analogous adducts $NiBr_2$(**Ia**) to $NiBr_2$(**Ic**) as light green powders (compounds **1**–**15**, eqn. 1). None of these compounds showed appreciable solubility in common organic solvents. In the expectation that replacing the phenyl substituents on the phosphorus atoms by methyl groups would lead to more soluble crystalline products, a similar series of reactions was conducted with the dimethylphosphino derivatives **II**, and with the 1,2-bis(iminophosphoranyl)ethane ligands **III** (R^1 = Ph) and **IV** (R^1 = Me). However, here, too, microcrystalline solids resulted, the poor solubility of which prevented purification by recrystallisation in most cases. Analytical and physical data for these complexes are collected in Table 1.

The complex $CoCl_2$(**Ic**) **5** was slightly more soluble in dichloromethane than the other compounds, and slow cooling of warm CH_2Cl_2 solutions yielded blue crystals of composition

Table 1 Analytical data for bis(iminophosphoranyl)alkane complexes, $MX_2\{(CH_2)_n(R_2P{=}NR')_2\}$

Compound	M	X	R	R′	*n*	Colour	Yield (%)	Found (Calc.) (%) C	H	N	P	X	$\tilde{\nu}_{P=N}$/cm^{-1}	μ_{eff}/μ_B
1	Co	Cl	Ph	mes	1	Light blue	95	65.4 (66.2)	5.6 (5.7)	3.5 (3.6)	7.1 (7.9)	10.8 (9.1)	1216	3.83
2	Ni	Br	Ph	mes	1	Light green	90	60.6 (59.4)	5.9 (5.1)	3.1 (3.2)	6.5 (7.1)	19.5 (18.4)	1211	3.34
3	Co	Cl	Ph	$C_6H_3Pr^i_2$	1	Light blue	93	65.1 (67.9)	6.5 (6.5)	4.0 (3.2)	6.3 (7.2)	10.0 (8.2)	1240	4.01
4	Ni	Br	Ph	$C_6H_3Pr^i_2$	1	Light green	95	61.1 (61.6)	3.6 (5.9)	3.0 (2.9)	6.7 (6.5)	17.3 (16.7)	1235	2.91
5	Co	Cl	Ph	Ph	1	Light blue	91	63.0 (63.8)	5.3 (4.5)	3.4 (4.0)	7.8 (8.9)	9.4 (10.2)	1242	3.93
6	Ni	Br	Ph	Ph	1	Aqua marine	88	56.8 (56.6)	4.5 (4.1)	3.2 (3.6)	6.9 (7.9)	18.5 (20.4)	1235	3.15
7	Co	Cl	Me	mes	1	Blue	78	51.9 (51.9)	6.9 (6.8)	5.0 (5.3)		13.1 (13.3)	1239	3.97
8	Ni	Br	Me	mes	1	Turquoise	93	44.0 (44.5)	6.0 (5.8)	3.1 (4.5)		25.5 (25.7)	1221	2.97
9	Co	Cl	Me	$C_6H_3Pr^i_2$	1	Blue	77	54.9 (56.5)	7.8 (7.9)	3.8 (4.5)	9.6 (10.1)	12.4 (11.5)	1245	3.91
10	Ni	Br	Me	$C_6H_3Pr^i_2$	1	Green	90	49.3 (49.3)	6.8 (6.9)	3.7 (4.0)	8.4 (8.9)	22.5 (22.6)	1239	2.61
11	Co	Cl	Ph	mes	2	Blue	78	65.6 (66.5)	6.0 (5.8)	2.6 (3.5)		8.6 (8.9)	1210	3.94
12	Co	Cl	Me	mes	2	Blue	80	51.6 (52.8)	6.9 (7.0)	4.6 (5.1)		12.4 (13.0)	1224	3.99
13	Ni	Br	Me	mes	2	Light green	77	43.8 (45.4)	6.1 (6.0)	3.7 (4.4)	9.2 (9.8)		1220	2.98
14	Co	Cl	Me	$C_6H_3Pr^i_2$	2	Green	87	58.7 (57.1)	8.3 (7.9)	4.2 (4.4)	10.2 (9.8)	10.5 (11.3)	1256	3.90
15	Ni	Br	Me	$C_6H_3Pr^i_2$	2	Light green	76	52.5 (50.9)	7.8 (7.1)	3.5 (4.0)	9.8 (8.8)	20.1 (22.9)	1248	3.73

mes = 2,4,6-$Me_3C_6H_2$.

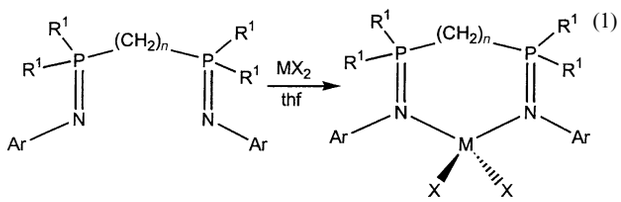

(1)

	M	X	*n*	R^1	Ar
1	Co	Cl	1	Ph	$C_6H_2Me_3$
2	Ni	Br	1	Ph	$C_6H_2Me_3$
3	Co	Cl	1	Ph	$C_6H_3Pr^i_2$
4	Ni	Br	1	Ph	$C_6H_3Pr^i_2$
5	Co	Cl	1	Ph	Ph
6	Ni	Br	1	Ph	Ph
7	Co	Cl	1	Me	$C_6H_2Me_3$
8	Ni	Br	1	Me	$C_6H_2Me_3$
9	Co	Cl	1	Me	$C_6H_3Pr^i_2$
10	Ni	Br	1	Me	$C_6H_3Pr^i_2$
11	Co	Cl	2	Ph	$C_6H_2Me_3$
12	Co	Cl	2	Me	$C_6H_2Me_3$
13	Ni	Br	2	Me	$C_6H_2Me_3$
14	Co	Cl	2	Me	$C_6H_3Pr^i_2$
15	Ni	Br	2	Me	$C_6H_3Pr^i_2$

5·3.5CH_2Cl_2 which proved suitable for X-ray diffraction. The structure is shown in Fig. 1; selected bond lengths and angles are given in Table 2. Compound **5** shows the expected chelate structure, with the two iminophosphoryl nitrogen atoms co-ordinated to tetrahedral cobalt, with Cl(1)–Co–Cl(2) and N(1)–Co–N(2) angles of 117.07(8) and 107.5(2)°, respectively. The Co–Cl and Co–N distances are unexceptional. The P=N bonds of, on average, 1.610(6) Å, are slightly longer than those of unco-ordinated $CH_2(Ph_2P{=}NC_6H_4Me\text{-}4)_2$ [1.568(2) Å],[7] whereas the P(1)–CH_2 bond in **5** is slightly shorter than in the "free" ligand [1.808(7) *vs.* 1.828(2) Å]. Comparable distances are found, for example, in the rhodium complex $[Rh\{CH_2(Ph_2P{=}NC_6H_4Me\text{-}4)_2\}(COD)]^+$.[8b] The P(1)–$CH_2$–P(2) angles, on the other hand, differ significantly between the cobalt complex **5** [122.1(4)°] and the rhodium congener [112.7(8)°]. The nitrogen atoms are trigonal planar, while the phosphorus atoms deviate only slightly from a tetrahedral structure.

The CP_2N_2Co six-membered ring adopts a comparatively flat boat conformation. One of the chloride ligands is in an axial position, while the other is shielded by the two phenyl substituents on the nitrogen atoms. The N-phenyl substituents are insufficiently bulky to form a protective co-ordination pocket around the metal centre; instead, they lie approximately parallel to the N(1)–Co–N(2) plane, obviously a consequence of their modest steric requirements.

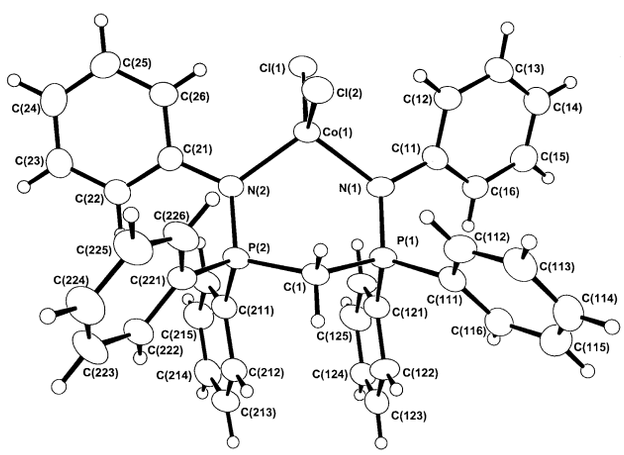

Fig. 1 Molecular structure of $CoCl_2\{CH_2(Ph_2P{=}NPh)_2\}$ **5**, showing the atomic numbering scheme. Ellipsoids are drawn at 40% probability level.

Bis(iminophosphoranyl)methanide complexes

Bis(iminophosphoranyl)methane is readily deprotonated by lithium amides, sodium hydride or lithium alkyls to give anions that are structurally related to acetylacetonate.[8e] Thus treatment of **Ia** with butyllithium in thf affords [**Ia** − H]$^-$ (Chart II). On addition of $NiBr_2$(dme) the pale yellow solution changes immediately to blue-green. Extraction with dichloromethane and cooling to −20 °C affords NiBr(**Ia** − H) **16** as a purple solid. The 2,6-diisopropylphenyl derivative NiBr(**Ib** − H) **17** is obtained as blue-purple crystals which are very soluble in dichloromethane and ethers but insoluble in hydrocarbons. The complexes are diamagnetic; in the case of **17** the square-planar geometry was confirmed by X-ray diffraction (see below). The green to blue-green cobalt complexes CoCl(**Ia** − H) **18** and CoCl(**Ib** − H) **19** were prepared in a similar fashion (eqn. 2), though in these cases crystals suitable for X-ray diffraction could not be obtained. The analytical data of these complexes are collected in Table 3.

Recrystallisation of complex **17** from dichloromethane yields purple crystals of **17**·CH_2Cl_2. The crystal structure is shown in Fig. 2. As the side view of this complex shows (Fig. 3), the nickel centre is strictly square-planar (angle sum 360.8°). The Ni–N distances of, on average, 1.9356(14) Å are very close to

Table 2 Selected bond lengths (Å) and angles (°)

$CoCl_2$(**Ic**)·3.5CH_2Cl_2 **5**·3.5CH_2Cl_2			
Co–Cl(1)	2.272(2)	Co–Cl(2)	2.277(2)
Co–N(1)	2.030(6)	Co–N(2)	2.034(6)
N(1)–C(11)	1.439(8)	N(1)–P(1)	1.606(6)
P(1)–C(1)	1.808(7)	P(2)–C(1)	1.819(8)
P(2)–N(2)	1.615(6)	P(1)–C(111)	1.796(7)
P(1)–C(121)	1.800(6)		
C(1)–Co–Cl(2)	117.07(8)	N(1)–Co–N(2)	107.5(2)
N(1)–Co–Cl(1)	107.0(2)	N(1)–Co–Cl(2)	107.2(2)
N(2)–Co–Cl(1)	111.7(2)	N(2)–Co–Cl(2)	106.0(2)
C(11)–N(1)–Co	117.4(4)	P(1)–N(1)–Co	121.2(3)
P(1)–N(1)–C(11)	119.3(5)	N(1)–P(1)–C(111)	112.4(3)
N(1)–P(1)–C(121)	116.4(3)	C(111)–P(1)–C(121)	110.3(3)
C(111)–P(1)–C(1)	103.4(3)	C(121)–P(1)–C(1)	105.6(3)
P(1)–C(1)–P(2)	122.1(4)	N(2)–P(2)–C(1)	108.8(3)
P(2)–N(2)–Co	119.5(3)	C(21)–N(2)–Co	119.7(4)
C(21)–N(2)–P(2)	118.0(5)		
NiBr(**Ib** − H)·CH_2Cl_2 **17**·CH_2Cl_2			
Ni–N(1)	1.9251(14)	Ni–N(5)	1.9461(14)
Ni–Br	2.3180(3)	Ni–C(3)	2.008(2)
N(1)–P(2)	1.6070(14)	P(4)–N(5)	1.6057(14)
P(2)–C(3)	1.761(2)	P(4)–C(3)	1.752(2)
N(1)–C(11)	1.431(2)	N(5)–C(51)	1.431(2)
P(2)–C(211)	1.801(2)	P(2)–C(221)	1.809(2)
C(3)–H(3)	0.92(2)		
N(1)–Ni–N(5)	158.30(6)	N(1)–Ni–C(3)	80.34(6)
N(5)–Ni–C(3)	81.33(6)	N(1)–Ni–Br	99.42(4)
N(5)–Ni–Br	99.71(4)	Br–Ni–C(3)	175.72(5)
C(11)–N(1)–P(2)	129.37(12)	C(11)–N(1)–Ni	135.84(11)
P(2)–N(1)–Ni	91.69(6)	N(1)–P(2)–C(3)	97.66(7)
P(2)–C(3)–P(4)	136.68(10)	P(2)–C(3)–Ni	84.63(7)
P(4)–C(3)–Ni	83.90(7)	P(2)–C(3)–H(3)	112.8(12)
P(4)–C(3)–H(3)	110.5(12)	Ni–C(3)–H(3)	102.9(12)
N(1)–P(2)–C(211)	116.59(8)	N(1)–P(2)–C(221)	113.37(8)
C(3)–P(2)–C(211)	111.05(8)	C(3)–P(2)–C(221)	114.14(8)
C(211)–P(2)–C(221)	104.41(8)	P(4)–N(5)–Ni	89.89(6)
Ni–N(5)–C(51)	132.36(11)	C(51)–N(5)–P(4)	131.01(11)
$FeBr_2$(**Vc**)·CH_2Cl_2 **24**·CH_2Cl_2			
Molecule 1			
Fe–N(6)	2.163(5)	Fe–N(2)	2.267(5)
Fe–N(1)	2.312(5)	Fe–Br(2)	2.4583(11)
Fe–Br(1)	2.4687(11)	N(1)–P(1)	1.559(6)
N(1)–Si(1)	1.747(6)	P(1)–C(1)	1.826(6)
P(2)–N(2)	1.574(5)	P(2)–C(5)	1.815(6)
Br(1)–Fe–Br(2)	128.75(4)	N(1)–Fe–N(2)	162.8(2)
N(1)–Fe–N(6)	81.8(2)	N(2)–Fe–N(6)	81.7(2)
N(1)–Fe–Br(1)	91.45(15)	N(1)–Fe–Br(2)	94.32(14)
N(2)–Fe–Br(1)	90.80(14)	N(2)–Fe–Br(2)	97.51(14)
N(6)–Fe–Br(1)	113.51(14)	N(6)–Fe–Br(2)	117.72(14)
P(1)–N(1)–Si(1)	126.1(3)	P(1)–N(1)–Fe	110.5(3)
Si(1)–N(1)–Fe	123.1(3)	N(1)–P(1)–C(1)	108.4(3)
P(1)–C(1)–N(6)	113.6(4)	C(5)–N(6)–Fe	119.7(4)
N(6)–C(1)–P(1)	113.6(4)	N(6)–C(5)–P(2)	114.6(4)
C(5)–P(2)–N(2)	107.5(3)	P(2)–N(2)–Fe	113.4(3)
P(2)–N(2)–Si(2)	122.3(3)	Si(2)–N(2)–Fe	124.0(3)
Molecule 2			
Fe–N(6)	2.159(5)	Fe–N(2)	2.233(5)
Fe–N(1)	2.340(6)	Fe–Br(1)	2.4388(11)
Fe–Br(2)	2.4771(11)	N(1)–P(1)	1.546(6)
N(1)–Si(1)	1.755(6)	P(1)–C(1)	1.838(6)
P(2)–N(2)	1.570(5)	P(2)–C(5)	1.833(6)
Br(1)–Fe–Br(2)	129.17(4)	N(1)–Fe–N(2)	161.6(2)
N(1)–Fe–N(6)	79.3(2)	N(2)–Fe–N(6)	82.4(2)
N(1)–Fe–Br(1)	93.8(2)	N(1)–Fe–Br(2)	89.0(2)
N(2)–Fe–Br(1)	95.97(13)	N(2)–Fe–Br(2)	96.80(14)
N(6)–Fe–Br(1)	115.38(14)	N(6)–Fe–Br(2)	115.00(14)
P(1)–N(1)–Si(1)	127.8(4)	P(1)–N(1)–Fe	113.1(3)
Si(1)–N(1)–Fe	119.0(3)	N(1)–P(1)–C(1)	107.3(3)
P(1)–C(1)–N(6)	114.5(4)	C(5)–N(6)–Fe	118.6(4)
N(6)–C(1)–P(1)	114.5(4)	N(6)–C(5)–P(2)	114.4(4)
C(5)–P(2)–N(2)	106.4(3)	P(2)–N(2)–Fe	110.7(3)
P(2)–N(2)–Si(2)	127.8(3)	Si(2)–N(2)–Fe	121.3(3)

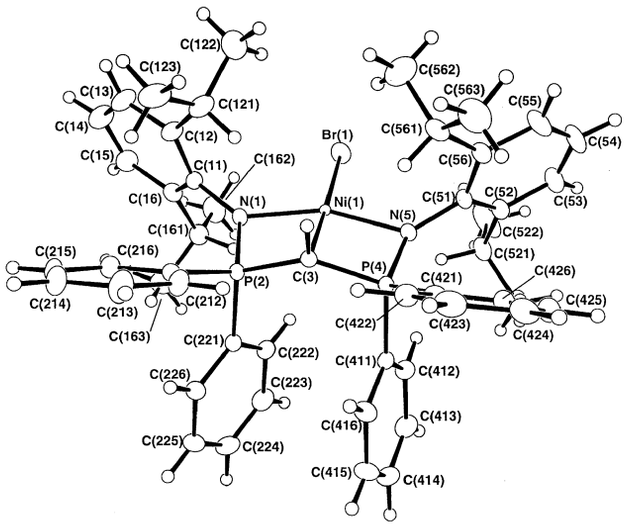

Fig. 2 Molecular structure of NiBr{$CH(Ph_2P{=}NC_6H_3Pr^i_2)_2$} **17**, showing the atomic numbering scheme.

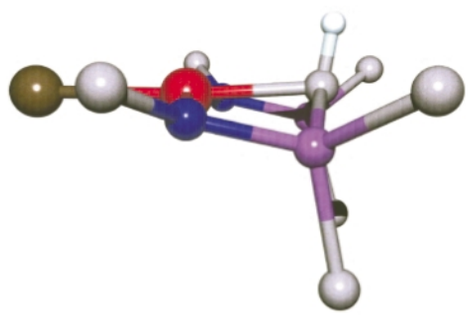

Fig. 3 Side view of complex **17**, showing the arrangement of the N_2P_2C ligand framework. The aryl substituents are omitted for clarity.

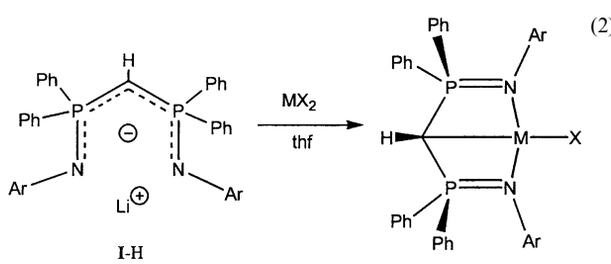

(2)

I-H

	M	X	Ar
16	Ni	Br	$C_6H_2Me_3$
17	Ni	Br	$C_6H_3Pr^i_2$
18	Co	Cl	$C_6H_2Me_3$
19	Co	Cl	$C_6H_3Pr^i_2$

Ni–N bond lengths in pyridine complexes, *e.g.* in $Ni(CH_2SiMe_3)_2(py)_2$ [1.957(8) Å][13] but shorter than in the tetrahedral diketimine complex $NiBr_2\{CH_2(MeC{=}NAr)_2\}$ [2.016(5) Å][3c] which shows also longer Ni–Br bonds than **17** [2.364(1) *vs.* 2.3180(3) Å]. Although the bis(iminophosphoranyl)methyl ligand in **17** is an anion for which a degree of charge delocalisation over the P=N bonds and hence a reduction in P=N bond order is usually formulated, as shown in Chart II, the P=N bonds in **17** are almost identical to those in **5**, 1.6064(14) Å on average. P=N bond lengths can vary significantly, from 1.51 Å in $[F_2P{=}N]_4$ and 1.645(4) Å in the $[P(NC_{10}H_7)_4]^{3-}$ anion[14] to single-bond values of *ca.* 1.77 Å.[15] The nitrogen atoms in **17** are almost trigonal-planar, angle sum 356.9°.

The fourth co-ordination site in complex **17** is occupied by a Ni–C(3) bond of 2.008(2) Å. Unusually, the atoms of the P_2CH moiety lie in one plane (angle sum of C(3) = 359.98°), while the

Table 3 Analytical data for bis(iminophosphoranyl)methanide complexes, $MX\{HC(Ph_2P{=}NR')_2\}$

Compound	M	R′	X	Colour	Yield (%)	Found (Calc.) (%) C	H	N	P	X
16	Ni	mes	Br	Purple	50	64.9 (65.5)	5.5 (5.3)	3.4 (3.6)	7.7 (7.9)	10.3 (10.1)
17	Ni	$C_6H_3Pr^i_2$	Br	Purple	52	68.4 (67.4)	6.2 (6.4)	3.6 (3.2)	7.7 (7.2)	10.3 (9.2)
18	Co	mes	Cl	Green-blue	52	69.1 (69.4)	6.8 (5.9)	3.4 (3.6)	7.5 (8.3)	4.3 (4.8)
19	Co	$C_6H_3Pr^i_2$	Cl	Green	56	69.3 (71.1)	6.4 (6.7)	2.7 (3.4)	8.9 (7.5)	5.9 (4.3)

Table 4 Comparison of geometric parameters of iminophosphorane complexes

Compound	*r*(P=N)/Å	*r*(P-CH)/Å	*r*(P-Ph)/Å	P-CH-P/°	P_2CH angle sum/°	Ref.
$CH_2(Ph_2P{=}NC_6H_4Me)_2$	1.568(2)	1.828(2)	av. 1.810(2)	115.2(1)		7
$[Rh\{CH_2(Ph_2P{=}NC_6H_4Me)_2\}(COD)]^+$	1.59(1)	1.85(1)	av. 1.81(1)	112.7(8)		8(*b*)
5	1.606(6)	1.808(7)	av. 1.800(6)	122.1(4)		[a]
17	av. 1.6064(14)	1.757(2)	av. 1.805(2)	136.68(10)	360	[a]
$TiCl_3\{C_2H_3(Ph_2P{=}NSiMe_3)_2\}$	1.604(4), 1.614(4)	1.775(4), 1.836(4)	av. 1.819(4)	123.8(3)	346	11(*a*)

[a] This work.

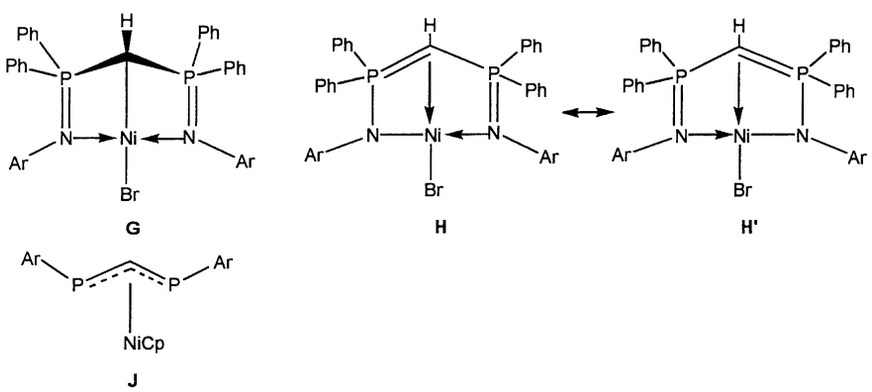

Ni–C(3)–H(3) angle is rather acute, 102.9(12)°. This geometry differs from the metal-bound carbon atoms in the C–N chelates $PtCl(PR_3)\{ArN{=}PPh_2C(Me)PPh_2{=}NAr\}$ [8e] and its rhodium congener,[8b] which are tetrahedral, and from $TiCl_3\{RN{=}PPh_2\text{-}CHCH_2PPh_2{=}NR\}$ (R = $SiMe_3$), which is halfway between tetrahedral and trigonal-planar (angle sum 346°).[11a] By contrast, the recently reported zinc and aluminium complexes $M\{HC(Ph_2P{=}NSiMe_3)_2\}$ (M = $AlMe_2$ or ZnMe) show no bonding between the metal and the CH-carbon atom.[16]

Equally unusual is the ^{13}C NMR chemical shift of the P–CH–P carbon atom in complex **17** which is found at δ −29.3, almost 60 ppm higher than for the related zinc complex.[16] The phosphorus–carbon coupling constants also differ distinctly, 108.5 Hz for **17** *versus* 120.6 Hz for the zinc compound. For these reasons the structure of **17** was subjected to a more detailed analysis.

The structure of complex **17** can, in principle, be described either by a σ-bond model (**G**), or as a delocalised system in which a P–CH–P heteroallyl moiety is π-bonded to the metal centre (**H**). A clear case for π-diphosphaallyl bonding exists, for example, in complex **J**, which contains a Ni–C(allyl) distance of 1.935(5) and short Ni–P^{III} bonds of 2.258(2) and 2.303(2) Å.[17] In **17** there are, of course, no bonding interactions between nickel and the tetrahedral phosphorus(v) atoms.

The question arises whether there is evidence for the participation of the delocalised bonding model **H**. As shown above, the P=N bond distances are a very poor criterion for charge delocalisation over the N_2P_2C ligand. A comparison of Ni–C bond lengths shows that these, too, are not clearly indicative. For example, nickel–alkyl σ bonds vary even in closely related complexes such as $Ni(CH_2SiMe_3)Cl(PMe_3)_2$ (1.95 Å) and $Ni(CH_2SiMe_3)_2(PMe_3)_2$ [2.08(2) Å].[18] Very similar Ni–C distances are found in a typical π complex, $Ni(\eta^3\text{-}C_3H_5)_2$ [Ni–C(1) 2.031, Ni–C(2) 1.980, Ni–C(3) 2.027 Å].[19]

The P–C(3) bonds of complex **17** [1.757(2) Å] are shorter than typical P–C σ bonds, *e.g.* to the phenyl substituents of the phosphorus atoms, but significantly longer than the P=C double bonds in the phosphorus ylids $Ph_3P{=}CH_2$ [1.662(8) Å][20] and $Me_3P{=}CHSiMe_3$ [1.653(11) Å, gas phase structure][21] and are consistent with some double-bond character. In order to facilitate structural comparisons, several pertinent geometric parameters for the "free" ligand $CH_2(Ph_2P{=}NC_6H_4Me\text{-}4)_2$ and a number of metal complexes are collected in Table 4. There is little variation in P=N bond lengths, and little structural evidence of significant participation of an amido structure as in **H**. On the other hand, the P–C(H) bond distances vary significantly as a function of the P–C–P angles. Wide P–C–P angles lead to shorter P–C bonds, as in the case of **17**; this is graphically represented in Fig. 4.

The bonding was further explored by single-point molecular orbital calculations using the LANL2MB basis set with pseudopotentials as defined in the GAUSSIAN 98 software package.[22] Calculations were based on the crystallographic co-ordinates. The Mulliken atomic charges obtained are shown in Fig. 5. Inclusion of all the aryl substituents led to significantly smaller charge separation than in a model where Ph was replaced by H. A visual inspection of all the orbitals in compound **17** reveals a large set of complex orbitals between the N_2P_2CH ligand and the nickel centre. This large number of orbitals disguises the presence of a distinct Ni–C bond. Representative orbitals are shown in Fig. 6 in order of increasing energy. A set of degenerate orbitals at −0.47 kcal mol^{-1} relative to the HOMO (not

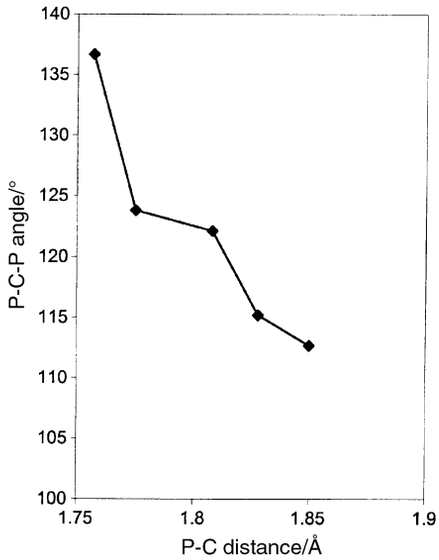

Fig. 4 Dependence of the P–C distance on the P–C–P angle in iminophosphorane complexes (*cf.* Table 4).

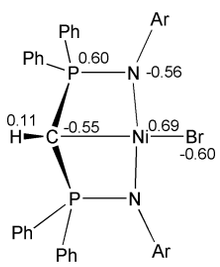

Fig. 5 Calculated Mulliken charge distribution in complex **17**.

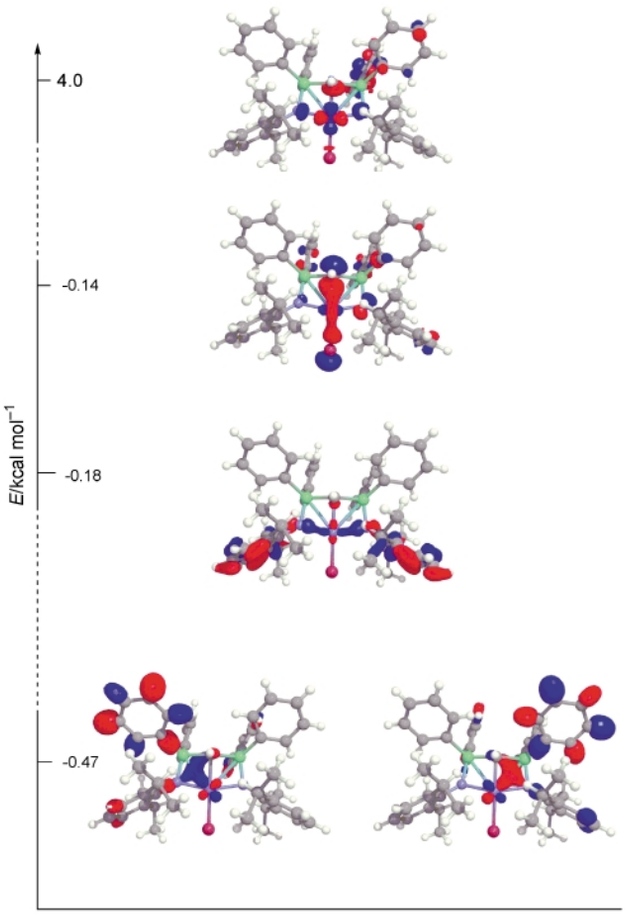

Fig. 6 Molecular orbitals of complex **17** involved in metal–ligand bonding.

shown[23]) illustrate the contribution of C–P–N charge delocalisation reflected in structures **H** and **H′**. The N–Ni–N bonding interaction is represented by a MO at −0.18 kcal mol^{-1}. The next highest bonding MO, at only very slightly higher energy, involves bonding of Ni to p-type orbitals of **C** and Br, *cf.* structure **G**. The LUMO (at +4.0 kcal mol^{-1}) is metal centred and Ni–C antibonding.

These considerations suggest that the bonding in complex **17** is best described by a mixture of the σ-bond model **G** and π-bonding contributions **H**. The C(3)–Ni bond in the trigonal-pyramidal P_2CHNi arrangement has presumably predominant p character.

2,6-Bis(aryliminophosphoranyl)pyridine complexes

The potentially tridentate ligands **V** and **VI** readily form adducts with a variety of metal halides (Scheme 2). Stirring a suspension of $VCl_3(thf)_3$ in dichloromethane with **Va** or **Vb** affords the corresponding VCl_3 adducts **20** and **21** as red microcrystalline solids which are poorly soluble in organic solvents. The reaction of FeX_2 with **Va** in thf at room temperature gives the adducts FeX_2(**Va**) as a grey powder (**22**, X = Cl) and a blue-grey microcrystalline solid (**23**, X = Br), respectively. Attempts to obtain crystals suitable for X-ray diffraction were not successful. By comparison, a similar reaction of the trimethylsilyl substituted ligand **Vc** with $FeBr_2$ gives the highly air- and moisture-sensitive complex **24** which is considerably more soluble. After standing in dichloromethane at room temperature for three days, dark violet crystals of **24**·CH_2Cl_2 were formed which were suitable for crystallographic studies.

Treatment of $CoCl_2$ with **Va**, **Vb** or **VIb** gave the corresponding $CoCl_2$ adducts in good yield as green crystals (**25**) or green microcrystalline powders (**27**, **29**). The analogous nickel dibromide complexes were obtained as pale red (**26**) or olive-green powders (**28**, **30**). The compounds are very sparingly soluble in toluene but, with the exception of **22**, dissolve well

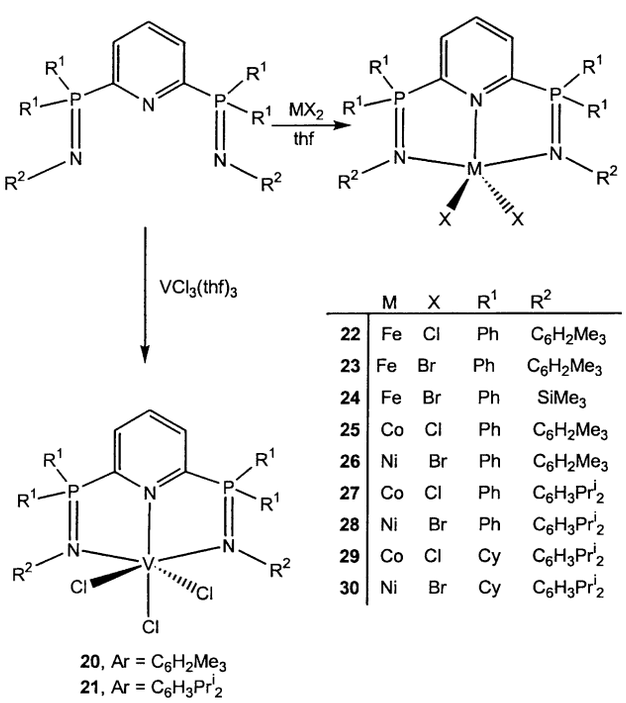

Scheme 2

in dichloromethane; **22**, **23** and **26** contain one molecule of CH_2Cl_2 of solvation.

The compounds are paramagnetic and were identified on the basis of their elemental analyses, infrared spectra, and FAB mass spectrometry. The data are collected in Table 5. Owing to their poor solubility, most compounds could not be purified

Table 5 Analytical data for bis(iminophosphoranyl)pyridine complexes, $MX_n\{C_5H_3N(R_2P{=}NR')_2\}$

Compound	M	X	*n*	Ligand	Colour	Yield (%)	Found (Calc.) (%) C	H	N	X	$\tilde{\nu}_{P=N}$/cm^{-1}	FAB-MS *m/z*
20	V	Cl	3	**Va**	Red	69	60.4 (60.3)	5.1 (5.0)	4.2 (4.4)	19.4 (18.5)	1198	834 (MLX_2^+)
21	V	Cl	3	**Vb**	Red	35	65.4 (66.6)	6.1 (6.0)	4.0 (4.4)	11.5 (11.1)	1177	954 (MLX_2^+)
22	Fe	Cl	2	**Va**	Grey	83	[a]62.7 (62.3)	5.1 (5.1)	4.2 (4.5)		1227	804 (MLX^+)
23	Fe	Br	2	**Va**	Blue-grey	63	[a]57.5 (56.8)	4.8 (4.7)	3.8 (4.1)		1222	N/O
24	Fe	Br	2	**Vc**	Dark violet	70	49.5 (50.2)	4.7 (4.9)	4.7 (5.0)	19.5 (19.1)		
25	Co	Cl	2	**Va**	Green	75	65.7 (66.9)	5.9 (5.4)	4.5 (5.0)	8.9 (8.4)	1225	807 (MLX^+)
26	Ni	Br	2	**Va**	Pale red	89	[a]56.9 (56.7)	5.0 (4.7)	4.0 (4.1)	17.5 (17.1)	1226	852 (MLX^+)
27	Co	Cl	2	**Vb**	Turquoise	74	68.3 (68.6)	6.8 (6.2)	4.3 (4.5)	7.8 (7.6)	1183	891 (MLX^+)
28	Ni	Br	2	**Vb**	Olive Green	89	58.3 (62.6)	5.7 (5.7)	3.9 (4.1)	17.2 (15.7)		936 (MLX^+)
29	Co	Cl	2	**VIb**	Green	72	65.6 (66.9)	8.7 (8.6)	3.7 (4.4)	7.2 (7.5)		N/O
30	Ni	Br	2	**VIb**	Olive green	79	62.0 (61.2)	8.3 (7.9)	3.7 (4.0)	15.9 (15.4)		N/O

[a] Contains one molecule CH_2Cl_2 of crystallisation.

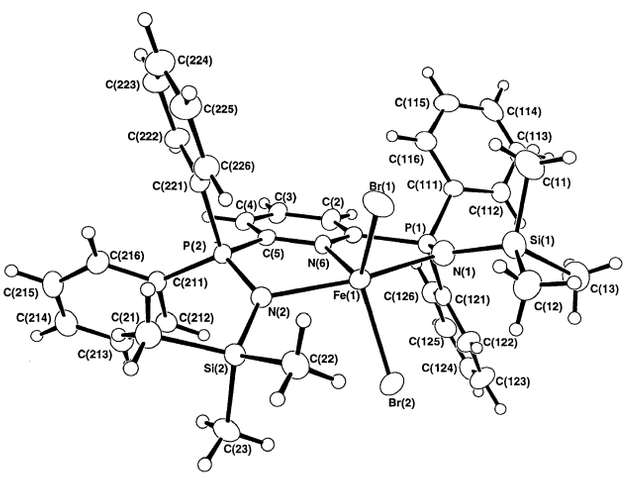

Fig. 7 Molecular structure of complex **24**, showing the atomic numbering scheme.

by recrystallisation, and this fact is reflected in some of the analytical values. However, in all cases the FAB mass spectra showed the expected $LMCl^+$ ions as the ions of highest mass ($LVCl_2^+$ in the case of vanadium). The infrared spectra show the expected P=N stretching frequencies at *ca.* 1180–1230 cm^{-1}. Compound **24** is sufficiently soluble for NMR studies; the ^{1}H NMR spectrum of this paramagnetic complex is consistent with a symmetrical tridentate co-ordination mode of **Vc** to the metal centre.

Preliminary X-ray diffraction data on complex **23** confirmed the tridentate co-ordination mode of ligand **Va** to $FeBr_2$. Although the basic complex geometry could be established, the crystals suffered from a high degree of mosaicity and did not refine satisfactorily. Better quality crystals were obtained on recrystallisation of **24** from dichloromethane. The molecular structure of **24**·CH_2Cl_2 is shown in Fig. 7. The iron centre is five-co-ordinate in an essentially trigonal-bipyramidal environment. There are two independent molecules in the unit cell. The bis(iminophosphino)pyridine framework is quite flexible, and the two conformations adopted by **24** in the solid state differ from one another in some interligand angles. For example, the angles N(6)–Fe–Br(1) and N(6)–Fe–Br(2) are different in molecule 1 [113.51(14) and 117.72(14)°] but almost identical in molecule 2. The $FeBr_2$ moiety in molecule 2 is more tilted with respect to the NNN plane than in molecule 1; as a consequence, the angles N(1)–Fe–Br(2) and N(2)–Fe–Br(2) in molecule 1 are quite similar [94.32(14) and 97.51(14)°, respectively] but differ by 7.8° in molecule 2.

A structural comparison of the P=N complex **24** with the related C=N complex $FeBr_2\{C_5H_3N(MeC{=}NAr)_2$-2,6} (Ar = 2,4,6-$Me_3C_6H_2$) is particularly instructive (Table 6). The latter is a highly active ethene polymerisation catalyst precursor.[4,24] The C=N bonds are *ca.* 0.28 Å shorter than P=N bonds, *i.e.* the P=N complex is sterically less strained. This has a number of structural consequences which appear to be crucial in terms of reactivity. In particular, the N–Fe–N angles for the *trans*-nitrogen atoms are 16.8° wider in **24** than in the C=N complex,[24] the Br–Fe–Br angle in **24** is 20° larger, and the tendency towards a square-pyramidal geometry that is quite pronounced in the iron and cobalt complexes of $C_5H_3N(MeC{=}NAr)_2$ ligands is absent in **24**.

Compared to $C_5H_3N(MeC{=}NAr)_2$, ligands of type **V** have a less extensive π system and should show reduced π-acceptor capacity. In an effort to quantify the difference in co-ordination strength, attempts were made to generate octahedral nickel(II) complexes of the N-phenyl derivative $C_5H_3N(Ph_2P{=}NPh)_2$-2,6 by treatment of $[Ni(H_2O)_6][BF_4]_2$ in acetonitrile. Under these conditions bis(imino)pyridines readily form octahedral 2:1 complexes $[NiL_2]^{2+}$ from which the crystal field splitting Δ_o is readily determined.[25] With $C_5H_3N(Ph_2P{=}NPh)_2$ there was no indication of complex formation under these conditions, and no bis(ligand) complexes could be obtained, an indication of the weaker co-ordination strength of iminophosphoranes compared to C=N analogues. On the other hand, modelling the $FeCl_2$ complexes **K** and **L** by *ab initio* calculations, including the

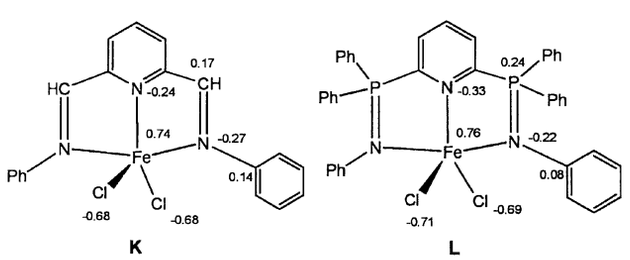

phenyl substituents, showed remarkably little difference in the charge distributions within these molecules. The pyridine nitrogen in **L** is slightly more negative than in **K**, and the P atoms are more positive than the corresponding C atoms in **K**. However, on the basis of these calculations the electronic differences between the two ligands appear to be less than is suggested by the differences in reactivity.

Polymerisation studies

A set of preliminary ethene polymerisation reactions was carried out in order to assess the effect of iminophosphorane ligands in catalyst systems. The cobalt complexes of bis(iminophophoranyl)alkanes and bis(iminophosphoranyl)pyridines such as **25**, **27** and **29** were activated with methylaluminoxane

Table 6 Comparison of bond distances (Å) and angles (°) of $(NN_2)FeBr_2$ complexes

	24		
	Molecule 1	Molecule 2	$FeBr_2\{C_5H_3N(MeC{=}NC_6H_2Me_3\text{-}2,4,6)_2\text{-}2,6\}$ [a]
Fe–N(py)	2.163(5)	2.159(5)	2.103(6)
Fe–N(imino)	2.312(5), 2.267(5)	2.340(6), 2.233(5)	2.271(6), 2.260(6)
Fe–Br(1)	2.4687(11)	2.4388(11)	2.452(2)
Fe–Br(2)	2.4583(11)	2.4771(11)	2.418(2)
N(1)–Fe–N(2)	162.8(2)	161.6(2)	145.4(3)
N(1)–Fe–Br(1)	91.45(15)	93.8(2)	102.5(2)
N(2)–Fe–Br(1)	90.80(14)	95.97(13)	98.3(2)
N(1)–Fe–Br(2)	94.32(14)	89.0(2)	97.0(2)
N(2)–Fe–Br(2)	97.51(14)	96.80(14)	102.0(2)
Br–Fe–Br	128.75(4)	129.17(4)	109.1(1)
N(py)–Fe–Br(2)	117.72(14)	115.00(14)	

[a] From ref. 24.

([MeAlO]$_n$, MAO) in toluene (Al : metal ratios 500 : 1 to 1000 : 1). Polymerisations were conducted at 50 °C at an ethene pressure of 10 bar. The complexes were all poorly soluble in toluene and even after reaction with MAO did not form a homogeneous solution. The actual amounts of dissolved catalysts are not known, which will have affected the catalytic performance. However, the activities found under these conditions were modest, with typical values of 5–30 kg polyethylene (PE) (mol metal)$^{-1}$ h^{-1} bar^{-1}. In all cases comparatively high molecular weight polymer was produced [M_w (1.5–4) × 10^5 g mol^{-1}]. The catalysts are relatively short-lived, and activity declines noticeably within 30 minutes. Mixtures of **17** and MAO (Al : Ni = 200 : 1) give a pale yellow solution. A negligible amount of ethene consumption was observed.

Particularly striking, in view of the high ethene polymerisation activities observed for catalysts based on iron complexes of the type $FeX_2\{C_5H_3N(MeC{=}NAr)_2\text{-}2,6\}$,[4,24] was the absence of ethene consumption by **22**–**24** under 1 bar ethene (50 °C). Again their use was hampered by their poor solubility in non-polar solvents. Similar to the bis(imino)pyridines, the P=N complexes form yellow solutions on addition of MAO; this is however not accompanied by ethene consumption. Similar negative results were obtained on activation of **23** with $AlClEt_2$, $AlBu^i_3/B(C_6F_5)_3$ or $AlBu^i_3/[CPh_3][B(C_6F_5)_3]$. At 10 bar/50 °C a mixture of $FeBr_2$ and **Vb** activated with MAO (Al:Fe = 1040 : 1) showed an activity of 6 × 10^3 g PE (mol Fe)$^{-1}$ h^{-1} bar^{-1}, with M_w = 382,000 and a polydispersity of 2.3.

The vanadium complexes show significantly higher activities. Adding an aliquot of a toluene solution of **21** to a MAO solution in toluene saturated with ethene (1 bar, Al : V = 500 : 1 to 1400 : 1) at room temperature results in immediate polymerisation. A ball of polymer is formed around the injected catalyst which, once formed, prevents further polymerisation. Here, too, the poor solubility of the catalyst precursor proved a problem and may be the reason for the rapid encapsulation of finely divided catalyst particles by polymer. Activities of up to 1.4 × 10^5 g PE (mol V)$^{-1}$ h^{-1} bar^{-1} were found under these conditions. The resulting polyethene proved to be very high molecular weight, and only 14–35% of the polymer was soluble in 1,2-dichlorobenzene at 140 °C. Size exclusion chromatography on the soluble part showed monomodal molecular weight distributions with $M_w = ca.$ 1.3 × 10^6 and M_w/M_n = 9–15. Bis(imino)pyridine vanadium complexes also give polyethylene with broad polydispersity but lower molecular weight.[26]

Conclusion

Bi- and tri-dentate iminophosphoranes with bulky substituents on the nitrogen atoms readily form chelate complexes with a variety of transition metals. Nickel bis(iminophosphoranyl)-methanide complexes show extensive charge delocalisation and, in contrast to comparable main group compounds, strong bonding to the methanide-carbon atom. Cobalt complexes of bis(iminophosphoranyl)alkanes possess modest ethene polymerisation activity, while 2,6-bis(iminophosphoranyl)pyridine complexes of iron(II) show only very low activity. By contrast, vanadium(III) complexes activated with MAO produce polyethene of very high molecular weight. In spite of the apparent similarity between P=N ligands and their C=N analogues, subtle electronic and steric changes lead to dramatic differences in reactivity.

Experimental

All manipulations were performed under dinitrogen using Schlenk techniques. Solvents were distilled under nitrogen over sodium–benzophenone (diethyl ether, thf), sodium (toluene), sodium–potassium alloy [light petroleum (bp 40–60 °C)], or CaH_2 (dichloromethane). NMR solvents were dried over activated 4A molecular sieves and degassed by several freeze–thaw cycles. NMR spectra were recorded using Bruker ARX250, DPX300 and DRX500 spectrometers. Chemical shifts are reported in ppm and referenced to residual solvent resonances (^{1}H, ^{13}C). ^{31}P NMR chemical shifts are relative to external 85% H_3PO_4. Aniline, 2,4,6-trimethylaniline, 2,6-diisopropylaniline, 2,6-difluoropyridine, bis(diphenylphosphino)methane, 1,2-bis-(diphenylphosphino)ethane, bis(dimethylphosphino)methane (dmpm), 1,2-bis(dimethylphosphino)ethane (dmpe) and dicyclohexylphosphine were used as purchased. Cobalt dichloride was purchased as anhydrous salt and dried further by extensive heating *in vacuo*. Phenyl azide was prepared as described.[27] The syntheses of ligands **Ia**, **Ib**–**IVa**, **IVb**, **Va**–**Vc** and **VIb** are given in the Electronic Supplementary Information.

Syntheses

Bis(aryliminophophoranyl)alkane complexes. *$CoCl_2\{CH_2(Ph_2P{=}NPh\}_2$* ***5***. A suspension of $CoCl_2$ (0.27 g, 2.1 mmol) in thf (50 cm^3) at room temperature was stirred with compound **Ic** (1.18 g, 2.1 mmol) overnight. A blue microcrystalline solid formed which was filtered off and dried to give a light blue powder. Yield 1.46 g (1.9 mmol, 91%). The complex is sparingly soluble in CH_2Cl_2. Crystals suitable for X-ray crystallography were grown by slowly cooling a warm solution of the complex in CH_2Cl_2.

$NiBr_2\{CH_2(Ph_2P{=}NPh\}_2$ ***6***. A suspension of $NiBr_2$·dme (0.55 g, 1.77 mmol) in thf was treated with a slight excess of **Ic** (1.00 g, 1.77 mmol) in thf at room temperature. The solution was stirred overnight and a green precipitate formed. The solvent was filtered off and the solid dried under vacuum. The

product was isolated as an aquamarine powder, yield 1.22 g (1.55 mmol, 88%).

Other complexes in the series **1**–**15** were prepared in an analogous manner as paramagnetic microcrystalline solids.

Complexes of the type MX[CH(PR′$_2$NR)$_2$]. *NiBr{CH(Ph$_2$P=NC$_6$H$_2$Me$_3$-2,4,6)$_2$}* ***16***. A solution of **Ia** (0.65 g, 0.92 mmol) in thf (50 cm^3) was cooled to −78 °C and treated with Bu^{n}Li (0.6 cm^3, 0.92 mmol). After stirring for 0.5 h and warming to room temperature, $NiBr_2$·dme (0.28 g, 0.92 mmol) was added and the solution stirred overnight to give a blue-green solution. The solvent was removed under vacuum, CH_2Cl_2 added and the resulting purple-blue solution filtered and kept at −20 °C overnight. A purple crystalline solid was isolated, yield 0.39 g (0.5 mmol, 50%). ^{1}H NMR (CD_2Cl_2, 20 °C): δ 7.77 (br s, 8 H, *m*-H of Ph), 7.39 (br s, 4 H, *p*-H of Ph), 7.38 (m, 8 H, *o*-H of Ph), 6.77 (bs, 4 H, *m*-H of mes), 2.81 (br s, 12 H, *o*-Me), 2.40 (bs, 6 H, *p*-Me) and 0.07 (vbs, 1 H, PCH). ^{13}C NMR ($CDCl_3$, 20 °C): δ 141.4 (s, *ipso*-C of Ph), 139.4 (s, *ipso*-C of mes), 134.2 (s, *o*-C of mes), 132.6 (s, *p*-C of Ph), 132.4 (s, *m*-C of Ph), 131.5 (s, *p*-C of mes), 129.0 (t, J_{CP} = 5.3 Hz, *o*-C of Ph), 128.0 (s, *m*-C of mes), 22.1 (s, *o*-Me) and 20.0 (s, *p*-Me). The P$_2$*C*H signal was not located. ^{31}P NMR ($CDCl_3$): δ 14.0.

NiBr{CH(Ph$_2$P=NC$_6$H$_2$Pr$^i_2$-2,6)$_2$} ***17***. Using the procedure given above, the complex was prepared from **Ib** (0.64 g, 0.87 mmol), Bu^{n}Li (0.55 cm^3, 0.92 mmol) and $NiBr_2$·dme (0.27 g, 0.87 mmol) as a purple crystalline solid, yield 0.40 g (0.46 mmol, 52%). ^{1}H NMR (CD_2Cl_2, 20 °C): δ 7.76 (br t, 8 H, J = 10.6, *m*-H of Ph), 7.43 (t, 4 H, J = 7.3, *p*-H of Ph), 6.77 (t, 8 H, J = 7.0, *o*-H of Ph), 6.92 (t, 2 H, J = 6.9, *p*-H of C$_6$H$_3$Pr$^i_2$), 6.83 (d, 4 H, J = 6.9, *m*-H of C$_6$H$_3$Pr$^i_2$), 4.03 (sept, 4 H, J = 6.8, C*H*Me$_2$), 1.59 (br d, 12 H, J = 4.4, CH*Me*$_2$), 0.98 (t, 1 H, J_{PH} = 4.4, PCHP) and 0.63 (br d, 12 H, J = 4.4 Hz, CH*Me*$_2$). ^{13}C NMR ($CDCl_3$, 20 °C): δ 147.1 (t, J_{CP} = 3.0, *o*-C of C$_6$H$_3$Pr$^i_2$), 137.2 (s, *ipso*-C of C$_6$H$_3$Pr$^i_2$), 133.1 (dd, J_{CP} = 93.7, 6.4, *ipso*-C of Ph), 132.3 (s, *p*-C of Ph), 130.9 (t, J_{CP} = 5.5, *m*-C of Ph), 128.8 (t, J_{CP} = 6.1, *o*-C of Ph), 124.0 (s, *p*-C of C$_6$H$_3$Pr$^i_2$) 123.4 (s, *m*-C of C$_6$H$_3$Pr$^i_2$), 29.5 (*C*HMe$_2$), 25.1 (CH*Me*$_2$), 23.2 (CH*Me*$_2$) and −29.3 (t, PCHP, J_{CP} = 108.5) Hz. ^{31}P NMR ($CDCl_3$): δ 20.9.

CoCl{CH(Ph$_2$P=NC$_6$H$_2$Me$_3$-2,4,6)$_2$} ***18***. A solution of **Ia** (0.55 g, 0.75 mmol) in thf (50 cm^3) was cooled to −78 °C and treated with Bu^{n}Li (0.47 cm^3, 0.75 mmol). After stirring for 0.5 h and warming to room temperature, $CoCl_2$ (0.097 g, 0.75 mmol) was added and the solution stirred overnight. A green powder was isolated, filtered off and dried, yield 0.29 g (0.39 mmol, 52%).

CoCl{CH(Ph$_2$P=NC$_6$H$_3$Pr$^i_2$-2,6)$_2$} ***19***. This was synthesized by the above procedure using **Ib** (0.64 g, 0.87 mmol), Bu^{n}Li (0.55 cm^3, 0.92 mmol) and $CoCl_2$ (0.11 g, 0.87 mmol) as a green powder, yield 0.40 g (0.48 mmol, 55%).

2,6-Bis(iminophosphoranyl)pyridine complexes. *VCl$_3${C$_5$H$_3$N(Ph$_2$P=NC$_6$H$_2$Me$_3$-2,4,6)$_2$-2,6}·CH$_2$Cl$_2$* ***20.*** A suspension of VCl_3(thf)$_3$ (0.450 g, 1.21 mmol) and **Va** (0.860 g, 0.88 mmol) in CH_2Cl_2 (20 cm^3) was stirred for 16 h, producing a brick red precipitate. The liquor was removed by filtration and the red solid dried under vacuum to give complex **20** (0.802 g, 0.84 mmol, 69%).

VCl$_3${C$_5$H$_3$N(Ph$_2$P=NC$_6$H$_3$Pr$^i_2$-2,6)$_2$-2,6} ***21***. From VCl_3(thf)$_3$ (0.468 g, 1.25 mmol) and **Vb** (1.0 g, 1.25 mmol) in CH_2Cl_2 (20 cm^3), red solid (0.420 g, 0.44 mmol, 35%).

FeCl$_2${C$_5$H$_3$N(Ph$_2$P=NC$_6$H$_2$Me$_3$-2,4,6)$_2$-2,6} ***22***. A suspension of $FeCl_2$ (0.089 g, 0.70 mmol) and **Va** (0.500 g, 0.70 mmol) in 30 cm^3 thf was stirred at ambient temperature for 24 h. Removal of the solvent resulted in a change from a red solution to a grey solid. The solid was washed with dichloromethane and dried (0.49 g, 0.58 mmol, 83%).

FeBr$_2${C$_5$H$_3$N(Ph$_2$P=NC$_6$H$_2$Me$_3$-2,4,6)$_2$-2,6} ***23***. This was synthesized by the above procedure, from $FeBr_2$ (0.151 g, 0.70 mmol) and **Va** (0.500 g, 0.70 mmol). Removal of thf left a grey solid which was recrystallised from hot dichloromethane to give a blue-grey crystalline solid (0.41 g, 0.44 mmol, 63%).

FeBr$_2${C$_5$H$_3$N(Ph$_2$P=NSiMe$_3$)$_2$-2,6} ***24***. A suspension of $FeBr_2$ (0.341 g, 1.58 mmol) and **Vc** (0.983, 1.58 mmol) was stirred at room temperature for 16 h. The solution was filtered, reduced in volume (10 cm^3) and layered with light petroleum. After standing at room temperature for 3 days, highly air and moisture sensitive dark violet crystals of complex **24** were formed which were suitable for crystallographic studies (0.87 g, 1.04 mmol, 66%). ^{1}H NMR (CD_2Cl_2, 20 °C): δ −0.24 (bs, 8 H, *o*-H of Ph), 1.93 (s, 4 H, *p*-H of Ph), 8.34 (s, 8 H, *m*-H of Ph), 15.11 (bs, 18 H, $SiMe_3$), 17.62 (bs, 1 H, *p*-H of py) and 83.59 (bs, 2 H, *m*-H of py).

CoCl$_2${C$_5$H$_3$N(Ph$_2$P=NC$_6$H$_2$Me$_3$-2,4,6)$_2$-2,6} ***25***. From $CoCl_2$ (0.092 g, 0.70 mmol) and **Va** (0.5 g, 0.70 mmol), as a green crystalline solid (0.44 g, 0.53 mmol, 75%).

NiBr$_2${C$_5$H$_3$N(Ph$_2$P=NC$_6$H$_2$Me$_3$-2,4,6)$_2$-2,6} ***26***. From $NiBr_2$·dme (0.22 g, 0.70 mmol) and **Va** (0.50 g, 0.70 mmol). The solvent was removed and the pale red solid residue washed with light petroleum and recrystallised from dichloromethane to give a red microcrystalline solid (0.58 g, 0.62 mmol, 89%).

CoCl$_2${C$_5$H$_3$N(Ph$_2$P=NC$_6$H$_3$Pr$^i_2$-2,6)$_2$-2,6} ***27***. From $CoCl_2$ (0.10 g, 0.75 mmol) and **Vb** (0.63 g, 0.75 mmol), as a green powder (0.52 g, 0.56 mmol, 74%).

NiBr$_2${C$_5$H$_3$N(Ph$_2$P=NC$_6$H$_3$Pr$^i_2$-2,6)$_2$-2,6} ***28***. Using the above procedure, treating $NiBr_2$·dme (0.25 g, 0.80 mmol) with **Vb** (0.64 g, 0.80 mmol) gave an olive green powder (0.73 g, 0.72 mmol, 90%).

CoCl$_2${C$_5$H$_3$N(Cy$_2$P=NC$_6$H$_3$Pr$^i_2$-2,6)$_2$-2,6} ***29***. This was synthesized by the above procedure using $CoCl_2$ (0.14 g, 1.09 mmol) and **VIb** (0.90 g, 1.09 mmol), as a green powder (0.72 g, 0.76 mmol, 72%).

NiBr$_2${C$_5$H$_3$N(Cy$_2$P=NC$_6$H$_3$Pr$^i_2$-2,6)$_2$-2,6} ***30***. This was synthesized by the above procedure using $NiBr_2$·dme (0.24 g, 0.77 mmol) and **VIb** (0.63 g, 0.77 mmol), as an olive green powder (0.63 g, 0.60 mmol, 79%).

Ethene polymerisations

Polymerisations at 1 bar are exemplified by the following procedure. To 15 mmol MAO in 50 cm^3 toluene saturated with 1 bar ethene at 20 °C was added a solution of complex **21** in toluene (2.5 cm^3, 27 μmol). Polymer precipitated immediately and impeded stirring. The reaction was terminated after 10 min by injection of methanol. The polymer was washed with acidified methanol and dried at 80 °C, yield 0.35 g.

MO calculations

The geometry obtained from the crystal structure of complex **17** was used in a single-point calculation using the LANL2MB basis set with pseudopotentials as defined in the GAUSSIAN 98 software package.[22] A Gaussian cube file was generated for each orbital, then surface contours were generated at 95%. Generated surfaces were ray-traced using POV-Ray. All computations were carried out on Pentium III class PCs running RedHat Linux. The structures of the iron complexes **K** and **L** were fully optimised, within the constraints of C_s symmetry.

X-Ray crystallography

In each case a suitable crystal was coated in an inert perfluoropolyether oil and mounted in a nitrogen stream at 150 K on a Nonius Kappa CCD area-detector diffractometer. Data collection was performed using Mo-Kα radiation (λ = 0.71073 Å) with the CCD detector placed 30 mm from the sample *via* a mixture of 1° ϕ and ω scans at different θ and κ settings using the program COLLECT.[28] The raw data were processed to produce conventional data using the program DENZO-SMN.[29] The datasets were corrected for absorption using the program

Table 7 Crystal data of iminophosphorane complexes

	5·3.5CH_2Cl_2	**17**·CH_2Cl_2	**24**·CH_2Cl_2
Formula	$C_{37}H_{32}Cl_2CoN_2P_2$·3.5CH_2Cl_2	$C_{50}H_{57}BrCl_2N_2NiP_2$	$C_{36}H_{43}Br_2Cl_2FeN_3P_2Si_2$
M	1690.07	957.44	922.42
Crystal system	Triclinic	Monoclinic	Triclinic
Space group	$P\bar{1}$	$P2_1/c$	$P\bar{1}$
a/Å	14.5550(8)	13.0035(1)	9.4409(2)
b/Å	15.5053(7)	21.2311(2)	20.1425(5)
c/Å	18.2403(9)	18.1551(1)	22.0698(5)
α/°	89.686(3)		79.8090(13)
β/°	91.7080(14)	107.9940(5)	79.5410(14)
γ/°	85.079(3)		88.6500(15)
U/Å^3	3807.1(3)	4767.08	4061.9(2)
Z	2	4	4
μ/mm^{-1}	0.953	1.460	2.638
Reflections collected/unique	47456/14209	77373/9352	66136/15808
R_{int}	0.1075	0.0106	0.0962
$R1[I > 2\sigma(I)]$	0.0974	0.0272	0.068
*wR*2 (all data)	0.2434	0.0702	0.1738

SORTAV.[30] All structures were solved by heavy-atom methods using SHELXS 97[31] and refined by full-matrix least squares (on F^2) using SHELXL 97.[32] All non-hydrogen atoms were refined with anisotropic displacement parameters. Hydrogen atoms were constrained to idealised positions. Crystallographic data for compounds **5**, **17** and **24** are summarised in Table 7.

CCDC reference number 186/2205.

See http://www.rsc.org/suppdata/dt/b0/b006329k/ for crystallographic files in .cif format.

Acknowledgements

We are grateful to the Engineering and Physical Sciences Research Council and BP Amoco Chemicals Ltd., Sunbury, for support (to S. A.-B. and M. J. S.).

References

1 G. J. P. Britovsek, V. C. Gibson and D. F. Wass, *Angew. Chem., Int. Ed.*, 1999, **38**, 428; R. R. Schrock, *Acc. Chem. Res.*, 1997, **30**, 9; S. D. Ittel, L. K. Johnson and M. Brookhart, *Chem. Rev.*, 2000, **100**, 1169; A. Michalak and T. Ziegler, *Organometallics*, 2000, **19**, 1850.

2 L. K. Johnson, C. M. Killian and M. Brookhart, *J. Am. Chem. Soc.*, 1995, **117**, 6414; C. M. Killian, D. J. Tempel, L. K. Johnson and M. Brookhart, *J. Am. Chem. Soc.*, 1996, **118**, 11664; S. J. McLain, J. Feldman, E. F. McCord, K. H. Gardner, M. F. Teasley, E. B. Coughlin, K. J. Sweetman, L. K. Johnson and M. Brookhart, *Macromolecules*, 1998, **31**, 6705; T. R. Bousiie, C. Coutard, H. Turner, V. Murphy and T. S. Powers, *Angew. Chem., Int. Ed.*, 1998, **37**, 3272.

3 (*a*) R. van Asselt, E. E. C. G. Dielens, R. E. Rulke, K. Vrieze and C. J. Elsevier, *J. Am. Chem. Soc.*, 1994, **116**, 977; (*b*) L. K. Johnson, S. Mecking and M. Brookhart, *J. Am. Chem. Soc.*, 1996, **118**, 267; (*c*) J. Feldman, S. J. McLain, A. Parthasarathy, W. J. Marshall, J. C. Calabrese and S. D. Arthur, *Organometallics*, 1997, **16**, 1514; (*d*) T. J. de Vries, R. Duchateau, M. A. G. Vorstman and J. T. F. Keurentjes, *Chem. Commun.*, 2000, 263.

4 A. M. A. Bennett, WO 98/27124 (DuPont), 1998; G. J. P. Britovsek, V. C. Gibson, B. S. Kimberley, P. J. Maddox, S. J. McTavish, G. A. Solan, A. J. P. White and D. J. Williams, *Chem. Commun.*, 1998, 849; B. L. Small, M. Brookhart and A. M. A. Bennett, *J. Am. Chem. Soc.*, 1998, **120**, 4049; C. Pellecchia, M. Mazzeo and D. Pappalardo, *Macromol. Rapid Commun.*, 1998, **19**, 651; B. L. Small and M. Brookhart, *Macromolecules*, 1999, **32**, 2120; E. A. H. Griffiths, G. J. P. Britovsek, V. C. Gibson and I. R. Gould, *Chem. Commun.*, 1999, 1333; K. Nomura, S. Warit and Y. Imanishi, *Macromolecules*, 1999, **32**, 4732.

5 C. M. Killian, L. K. Johnson and M. Brookhart, *Organometallics*, 1997, **16**, 2005; B. L. Small and M. Brookhart, *J. Am. Chem. Soc.*, 1998, **120**, 7143; S. Plentz Meneghetti, P. J. Lutz and J. Kress, *Organometallics*, 1999, **18**, 2734.

6 W. Keim, R. Appel, A. Storeck, C. Krüger and R. Goddard, *Angew. Chem., Int. Ed. Engl.*, 1981, **20**, 116. For recent examples of NPN chelates as polymerisation catalysts see R. Vollmerhaus, P. Shao, N. J. Taylor and S. Collins, *Organometallics*, 1999, **18**, 2731.

7 P. Imhoff, R. van Asselt, C. J. Elsevier, K. Vrieze, K. Goubitz, K. F. van Malssen and C. H. Stam, *Phosphorus, Sulfur Silicon Relat. Elem.*, 1990, **147**, 401.

8 (*a*) P. Imhoff and C. J. Elsevier, *J. Organomet. Chem.*, 1989, **361**, C61; (*b*) P. Imhoff, R. van Asselt, C. J. Elsevier, M. C. Zoutberg and C. H. Stam, *Inorg. Chim. Acta*, 1991, **184**, 73; (*c*) M. W. Avis, K. Vrieze, H. Kooijman, N. Veldman, A. L. Spek and C. J. Elsevier, *Inorg. Chem.*, 1995, **34**, 4092; (*d*) M. W. Avis, C. J. Elsevier, N. Veldman, H. Kooijman and A. L. Spek, *Inorg. Chem.*, 1996, **35**, 1518; (*e*) M. W. Avis, K. Vrieze, J. M. Ernsting, C. J. Elsevier, N. Veldman, A. L. Spek, K. V. Katti and C. L. Barnes, *Organometallics*, 1996, **15**, 2376; (*f*) M. W. Avis, M. Goosen, C. J. Elsevier, N. Veldman, H. Kooijman and A. L. Spek, *Inorg. Chim. Acta*, 1997, **264**, 43.

9 D. M. Hankin, A. A. Danopoulos, G. Wilkinson, T. K. N. Sweet and M. B. Hursthouse, *J. Chem. Soc., Dalton Trans.*, 1996, 4063; L. R. Falvello, S. Fernandez, M. M. Garcia, R. Navarro and E. P. Urriolabeita, *J. Chem. Soc., Dalton Trans.*, 1998, 3745.

10 K. V. Katti, B. D. Santarsiero, A. A. Pinkerton and R. G. Cavell, *Inorg. Chem.*, 1993, **32**, 5919; R. W. Reed, B. Santarsiero and R. G. Cavell, *Inorg. Chem.*, 1996, **35**, 4292; R. S. Pangurangi, K. V. Katti, L. Stillwell and C. L. Barnes, *J. Am. Chem. Soc.*, 1998, **120**, 11364; J. Vincente, A. Arcas, D. Batista and M. C. R. de Arellano, *Organometallics*, 1998, **17**, 4544.

11 (*a*) M. J. Sarsfield, M. Thornton-Pett and M. Bochmann, *J. Chem. Soc., Dalton Trans.*, 1999, 3329; (*b*) see also P. B. Hitchcock, M. F. Lappert, P. G. H. Uiterweerd and Z. X. Wang, *J. Chem. Soc., Dalton Trans.*, 1999, 3413.

12 H. Christina, E. McFarlane and W. McFarlane, *Polyhedron*, 1988, **7**, 1875; H. Christina, E. McFarlane, W. McFarlane and A. S. Muir, *Polyhedron*, 1990, **9**, 1757.

13 E. Carmona, F. Gonzalez, M. L. Poveda, J. L. Atwood and R. D. Rogers, *J. Chem. Soc., Dalton Trans.*, 1981, 777.

14 P. R. Raithby, C. A. Russell, A. Steiner and D. S. Wright, *Angew. Chem., Int. Ed. Engl.*, 1997, **36**, 649.

15 N. N. Greenwood and A. E. Earnshaw, *Chemistry of the Elements*, 2nd edn., Butterworth, Oxford, 1997, p. 531ff.

16 K. Aparna, R. McDonald and R. G. Cavell, *Organometallics*, 1999, **18**, 3775; K. Aparna, R. McDonald, M. Ferguson and R. G. Cavell, *Organometallics*, 1999, **18**, 4241.

17 R. Appel, W. Schuhn and E. Knoch, *J. Organomet. Chem.*, 1987, **319**, 345.

18 E. Carmona, M. Paneque, M. L. Poveda, R. D. Rogers and J. L. Atwood, *Polyhedron*, 1984, **3**, 317.

19 R. Goddard, C. Krüger, F. Mark, R. Stansfield and X. Zhang, *Organometallics*, 1985, **4**, 285.

20 J. C. J. Bart, *J. Chem. Soc. B*, 1969, 350.

21 E. A. V. Ebsworth, D. W. H. Rankin, B. Zimmer-Gasser and H. Schmidbaur, *Chem. Ber.*, 1980, **113**, 1637.

22 GAUSSIAN 98, Revision A. 7. M. J. Frisch, G. W. Trucks, H. B. Schlegel, G. E. Scuseria, M. A. Robb, J. R. Cheeseman, V. G. Zakrzewski, J. A. Montgomery, Jr., R. E. Stratmann, J. C. Burant, S. Dapprich, J. M. Millam, A. D. Daniels, K. N. Kudin, M. C. Strain, O. Farkas, J. Tomasi, V. Barone, M. Cossi, R. Cammi, B. Mennucci, C. Pomelli, C. Adamo, S. Clifford, J. Ochterski, G. A. Petersson, P. Y. Ayala, Q. Cui, K. Morokuma, D. K. Malick, A. D. Rabuck, K. Raghavachari, J. B. Foresman, J. Cioslowski, J. V. Ortiz, A. G. Baboul, B. B. Stefanov, G. Liu, A. Liashenko, P. Piskorz,

I. Komaromi, R. Gomperts, R. L. Martin, D. J. Fox, T. Keith, M. A. Al-Laham, C. Y. Peng, A. Nanayakkara, C. Gonzalez, M. Challacombe, P. M. W. Gill, B. Johnson, W. Chen, M. W. Wong, J. L. Andres, C. Gonzalez, M. Head-Gordon, E. S. Replogle and J. A. Pople, Gaussian, Inc., Pittsburgh, PA, 1998.
23 The HOMO in this molecule is formed by the non-bonding electron pairs of the bromide ligand.
24 G. J. P. Britovsek, M. Bruce, V. C. Gibson, B. S. Kimberley, P. J. Maddox, S. Mastroianni, S. J. McTavish, C. Redshaw, G. A. Solan, S. Strömberg, A. J. P. White and D. Williams, *J. Am. Chem. Soc.*, 1999, **121**, 8728.
25 E. C. Alyea and P. H. Merrell, *Inorg. Chim. Acta*, 1978, **28**, 91.
26 D. Reardon, F. Conan, S. Gambarotta, G. Yap and Q. Wang, *J. Am. Chem. Soc.*, 1999, **121**, 9318.
27 I. Ugi, H. Perlinger and L. Behringer, *Chem. Ber.*, 1958, **91**, 2330.
28 COLLECT, data collection software, Nonius B.V., Delft, 1999.
29 Z. Otwinowski and W. Minor, *Methods Enzymol.*, 1996, **276**, 307.
30 R. H. Blessing, *Acta Crystollogr.*, *Sect. A*, 1995, **51**, 33.
31 G. M. Sheldrick, *Acta Crystallogr.*, *Sect. A*, 1990, **46**, 467.
32 G. M. Sheldrick, SHELXL 97, Program for crystal structure refinement, University of Göttingen, 1997.